

# Dose-Dependent Scavenging of Methylglyoxal by Naringenin in Diabetic Mice

Xinxin Huang, Huixian Zhou, Ting Tan,<sup>\*,§</sup> and Yun Luo<sup>\*,§</sup>



Cite This: *ACS Omega* 2025, 10, 18615–18621



Read Online

ACCESS |



Metrics & More

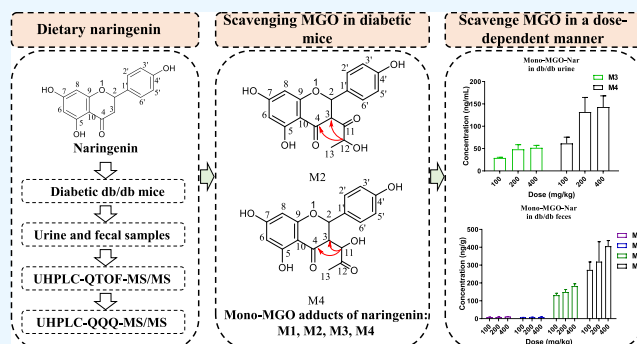


Article Recommendations



Supporting Information

**ABSTRACT:** Methylglyoxal (MGO) has driven interest as a major precursor of advanced glycation end products due to it being closely implicated in the pathogenesis of diabetic kidney disease (DKD). Therefore, it is critical for seeking active scavenger-targeted MGO to mitigate the development of DKD. Previous studies demonstrated that naringenin (Nar) has a remarkable therapeutic effect on DKD. However, whether Nar could scavenge MGO in diabetic mice remains virtually unknown. This work aims to investigate the effect and mechanism of scavenging MGO by Nar in diabetic mice. Liquid chromatography coupled to tandem mass spectrometry (LC–MS/MS) was applied for investigating the scavenging capacity and mechanism of Nar on MGO in diabetic mice. The results indicated that Nar could significantly scavenge MGO in diabetic mice based on the formation of mono-MGO–Nar. In addition, two mono-MGO–Nar nanoparticles were purified, and their structures were deduced as 3-MGO–Nar using LC–MS/MS and NMR spectroscopic analyses. Furthermore, the dose-dependent scavenge effect of Nar on MGO in diabetic mice was elucidated by quantifying mono-MGO–Nar in urine and feces using LC–MS/MS. In summary, our results first demonstrated that targeting the MGO burden may be the new mechanism of Nar combating DKD.



## INTRODUCTION

Diabetic kidney disease (DKD) as the major complication of diabetic patients is a significant risk for public health.<sup>1–3</sup> Higher plasma levels of methylglyoxal (MGO) were detected in diabetic patients than that in healthy people because of endogenous production from the pathway of glucose glycolysis, which led to increased formation of advanced glycation end products (AGEs).<sup>4–6</sup> Numerous studies have demonstrated that MGO and MGO-derived AGEs play pivotal roles in the pathogenesis of DKD.<sup>7–9</sup> Therefore, there is a critical need for diabetic patients to alleviate DKD by seeking MGO scavengers. The flavonoids,<sup>10,11</sup> as the major MGO scavengers, have been uncovered by Professor Shengmin Sang's research group based on the C6 and C8 of the A ring reacted with MGO to form the mono-MGO or di-MGO adducts, which were excreted by the urine and feces of mice and humans.<sup>12–21</sup> Thus, flavonoids are worth further exploring to combat DKD by scavenging MGO.<sup>22</sup>

Naringenin (Nar) belonging to the flavanone subclass, is widely distributed in citrus fruits and herbs, which has been reported to exhibit a significant therapeutic effect on DKD with respect to anti-inflammatory, antifibrotic, and antioxidant properties.<sup>23–26</sup> A study indicated that Nar could react with MGO in vitro.<sup>27</sup> Therefore, we proposed the hypothesis that Nar showed a significant therapeutic effect on DKD by reducing MGO stress.

To confirm the above hypothesis, the content of this study can be summarized as follows: (1) the scavenging effect and mechanism of Nar on MGO in diabetic mice was investigated by liquid chromatography coupled to tandem mass spectrometry (LC–MS/MS). (2) Phytochemical analysis of reaction between Nar and MGO in vitro yielded two mono-MGO–Nar, for which the structures were elucidated by 1D and 2D NMR experiments. (3) The scavenging ability of Nar on MGO was further investigated based on quantification of mono-MGO–Nar by LC–MS/MS.

## RESULTS AND DISCUSSION

**Evaluation of MGO Scavenging Capacity and Mechanism by Nar In Vitro.** The experimental results in this paper showed that as time increased, the scavenging capacity of MGO by Nar also increased, with a capture rate of up to 72.34% after reaction for 8 h (Figure 1A).

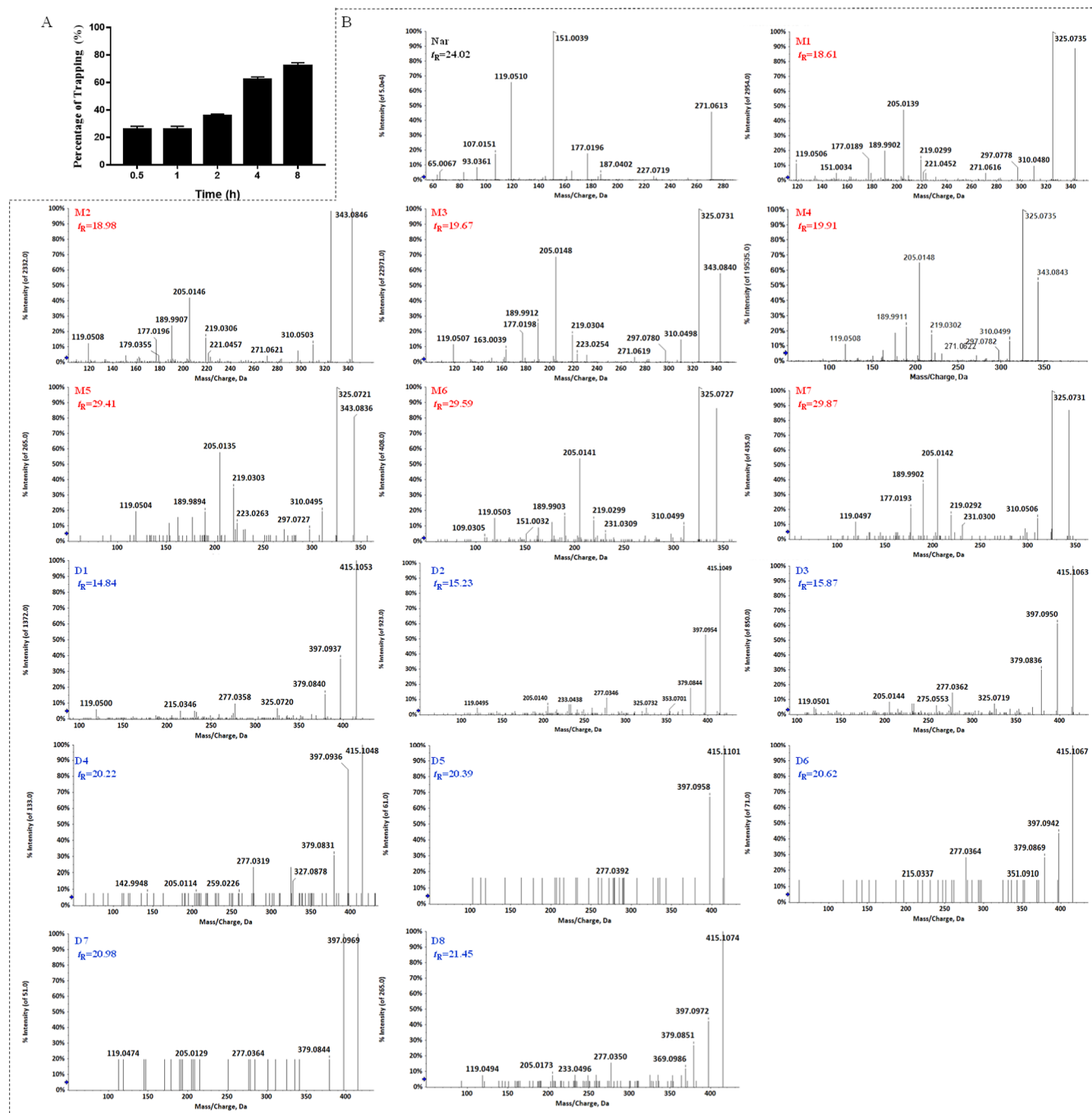
**Received:** December 19, 2024

**Revised:** April 2, 2025

**Accepted:** April 25, 2025

**Published:** April 30, 2025



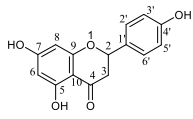
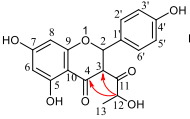
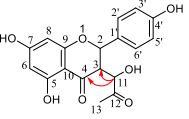


**Figure 1.** Scavenging effect and mechanism of MGO by Nar in vitro. (A) The percentage of scavenging MGO (0.4 mM) by Nar (1.2 mM) at different incubation times (data are shown as means  $\pm$  SD,  $n = 3$ ). (B) The MS/MS spectra of mono-MGO-Nar, di-MGO-Nar, and Nar identified in the reaction mixture between Nar and MGO at 8 h.

The retro-Diels–Alder (RDA) fragmentation on the C ring of Nar with the formula of  $C_{15}H_{12}O_5$  (retention time (RT) = 24.02 min) based on retrocyclization cleavages yielded characteristic fragment ions (CFIs)  $m/z$  151.0037 and  $m/z$  119.0502 as the main fragmentation process, which was used for identification of reaction products between Nar and MGO (Figure S1). Seven peaks at 18.61 (M1), 18.98 (M2), 19.67 (M3), 19.91 (M4), 29.41 (M5), 29.59 (M6), and 29.87 min (M7) with precursor ion  $m/z$  343.0823 and the formula of  $C_{18}H_{16}O_7$  had CFI  $m/z$  271.0612 (Nar) resulted from neutral loss (NL) of MGO ( $C_3H_4O_2$ , 72 Da). These seven peaks were further identified as mono-MGO adducts of Nar due to CFIs

$m/z$  151.0037 and  $m/z$  119.0502 observed in the MS/MS spectra. Theoretically, RDA on the C ring of flavonoids could be applied for differentiating the reaction ring of MGO on Nar. Unfortunately, similar fragmentation patterns of mono-MGO-Nar were found (Figure 1B), which indicated that it was difficult to distinguish the reaction ring of MGO on Nar. Peaks at 14.84 (D1), 15.23 (D2), 15.87 (D3), 20.22 (D4), 20.39 (D5), 20.62 (D6), 20.98 (D7), and 21.45 min (D8) ( $m/z$  415.1077,  $[M - H]^-$ ) with the formula of  $C_{21}H_{20}O_9$  yielded CFIs  $m/z$  343.0823 (mono-MGO-Nar) and  $m/z$  271.0612 (Nar) by continuous NL of MGO ( $C_3H_4O_2$ , 72 Da). Peaks at 14.84, 15.23, 15.87, 20.22, 20.39, 20.62, 20.98, and 21.45 min

Table 1. Structures and  $^1\text{H}$  (600 MHz) and  $^{13}\text{C}$  (150 MHz) NMR Data of Nar, M2, and M4 in  $\text{DMSO}-d_6$  ( $\delta$  in ppm)

No.						
	$\delta_{\text{H}}$ (ppm)	$\delta_{\text{C}}$ (ppm)	$\delta_{\text{H}}$ (ppm)	$\delta_{\text{C}}$ (ppm)	$\delta_{\text{H}}$ (ppm)	$\delta_{\text{C}}$ (ppm)
1	—	—	—	—	—	—
2	5.44 dd	78.40	5.39 d	80.48	5.33 d	81.80
3	2.70 dd/3.27 dd	42.44	3.71 dd	53.86	3.90 dd	54.67
4	—	196.30	—	196.27	—	195.45
5	—	163.5	—	163.91	—	163.93
6	5.89 s	96.80	5.85 d	95.41	5.86 d	96.41
7	—	166.70	—	167.40	—	167.40
8	5.89 s	95.00	5.90 d	95.41	5.89 d	95.41
9	—	162.90	—	163.10	—	163.07
10	—	101.70	—	102.16	—	102.29
11	—	—	—	212.33	3.39 d	73.59
12	—	—	4.59 dd	73.01	—	211.26
13	—	—	1.62 s	25.99	2.20 s	26.47
1'	—	128.80	—	127.40	—	127.80
2'	7.32 d	128.20	7.20 d	130.57	7.39 d	129.80
3'	6.79 d	115.10	6.71 d	115.23	6.82 d	115.75
4'	—	157.70	—	158.45	—	158.53
5'	6.79 d	115.10	6.71 d	115.23	6.82 d	115.75
6'	7.32 d	128.20	7.20 d	130.57	7.39 d	129.80

no	$\delta_{\text{H}}$ (ppm)	$\delta_{\text{C}}$ (ppm)	$\delta_{\text{H}}$ (ppm)	$\delta_{\text{C}}$ (ppm)	$\delta_{\text{H}}$ (ppm)	$\delta_{\text{C}}$ (ppm)
1						
2	5.44 dd	78.40	5.39 d	80.48	5.33 d	81.80
3	2.70 dd/3.27 dd	42.44	3.71 dd	53.86	3.90 dd	54.67
4		196.30		196.27		195.45
5		163.5		163.91		163.93
6	5.89 s	96.80	5.85 d	95.41	5.86 d	96.41
7		166.70		167.40		167.40
8	5.89 s	95.00	5.90 d	95.41	5.89 d	95.41
9		162.90		163.10		163.07
10		101.70		102.16		102.29
11				212.33	3.39 d	73.59
12			4.59 dd	73.01		211.26
13			1.62 s	25.99	2.20 s	26.47
1'		128.80		127.40		127.80
2'	7.32 d	128.20	7.20 d	130.57	7.39 d	129.80
3'	6.79 d	115.10	6.71 d	115.23	6.82 d	115.75
4'		157.70		158.45		158.53
5'	6.79 d	115.10	6.71 d	115.23	6.82 d	115.75
6'	7.32 d	128.20	7.20 d	130.57	7.39 d	129.80

were further identified as di-MGO adducts of Nar by the CFIs  $m/z$  151.0037 and  $m/z$  119.0502 (Figure 1B). According to the reported literature,<sup>28</sup> we found that flavonoids can capture MGO at the same reaction site to form two isomeric products. Therefore, Nar can react with MGO to produce seven mono-MGO adducts and eight di-MGO adducts.

**Structural Elucidation of Isolated Reaction Products from the System of Nar and MGO In Vitro.** As shown in Table 1, the  $^1\text{H}$  NMR spectrum of M2 and M4 was similar to Nar. The major difference was the extra signals at  $\delta_{\text{H}}$  4.59 (1H, dd) and  $\delta_{\text{H}}$  1.62 (3H, s) for M2 and at  $\delta_{\text{H}}$  3.39 (1H, d) and  $\delta_{\text{H}}$

2.20 (3H, s) for M4, which were assigned to the MGO residue. M2 had only one proton signal on C3 at  $\delta_{\text{H}}$  3.71 (1H, dd) instead of two proton signals at  $\delta_{\text{H}}$  2.70 (1H, dd) and  $\delta_{\text{H}}$  3.27 (1H, dd) on Nar (Figure S2). The  $^{13}\text{C}$  NMR spectra showed that M2 had  $\delta_{\text{C}}$  53.86 (C3) instead of  $\delta_{\text{C}}$  42.44 (C3) on Nar (Figure S3), suggesting that MGO conjugated with Nar at position C3 of the C ring. Furthermore, HMBC correlations were found between the proton at  $\delta_{\text{H}}$  4.59 (H12) and the carbons at  $\delta_{\text{C}}$  53.86 (C3) and  $\delta_{\text{C}}$  196.27 (C4), which indicated the MGO group was connected to the C3 position of the C ring (Figure S4). In addition, one proton signal on C3 at  $\delta_{\text{H}}$

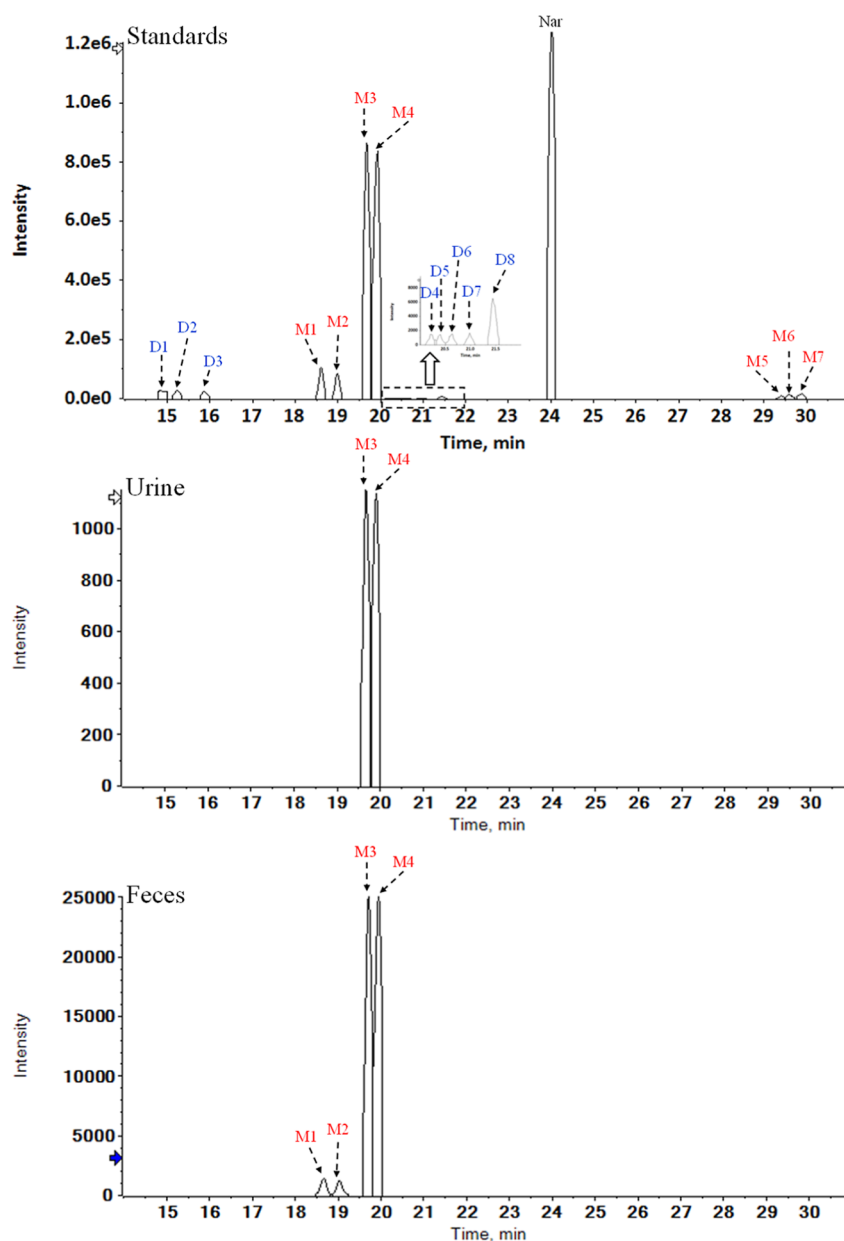


**Figure 2.** Extracted ion chromatograms (EICs) of identified reaction products between Nar and MGO at 8 h and mono-MGO-Nar in urine and fecal samples of diabetic mice after oral administration of Nar.

3.90 (1H, dd) of M4 instead of two proton signals at  $\delta_{\text{H}}$  2.70 (1H, dd) and  $\delta_{\text{H}}$  3.27 (1H, dd) on Nar was observed (Figure S5). M4 had  $\delta_{\text{C}}$  54.67 (C3) instead of  $\delta_{\text{C}}$  42.44 (C3) on Nar (Figure S6), suggesting that MGO conjugated with Nar at position C3 of the C ring. Furthermore, HMBC correlations between the proton at  $\delta_{\text{H}}$  3.39 (H11) and the carbons at  $\delta_{\text{C}}$  54.67 (C3) and  $\delta_{\text{C}}$  195.45 (C4),  $\delta_{\text{H}}$  2.20 (H13) and  $\delta_{\text{C}}$  73.59 (C-11), indicated the MGO group was connected to the C3 position of the C ring (Figure S7).  $^1\text{H}$ – $^1\text{H}$  COSY correlation (Figure S8) between H11 and H3 was observed. The HSQC spectrum correlation of M4 indicated that the carbons at  $\delta_{\text{C}}$  73.59 (C-11) and the protons at  $\delta_{\text{H}}$  3.39 (1H, d),  $\delta_{\text{C}}$  26.47 (C-13), and  $\delta_{\text{H}}$  2.20 (3H, s) were directly connected (Figure S9). Thus, M2 and M4 were characterized as 3-MGO-Nar.

**Scavenging Mechanism of Nar on MGO in Diabetic Mice.** The four mono-MGO adducts of Nar (RT = 18.65, 19.08, 19.73, and 19.97 min) were identified as M1, M2, M3

and M4 in feces by comparing RT and MS/MS spectra of reaction products between Nar and MGO in vitro (Figure S10), and high contents of two M3 and M4 adducts were also found in urine. The extracted ion chromatograms (EICs) of identified reaction products between Nar and MGO at 8 h and mono-MGO-Nar in urine and fecal samples of diabetic mice after oral administration of Nar were presented in Figure 2. The results indicated that Nar could significantly scavenge MGO in diabetic mice.

**Method Validation.** The standard curves of M2 and M4 in mice urine displayed superior linearity ranging from 1 to 1000 ng/mL (M2 in the db/db urine:  $y = 0.1301x + 0.9371$ ,  $R^2 = 0.9929$ ; M4 in the db/db urine:  $y = 0.1762x + 3.548$ ,  $R^2 = 0.9949$ ), where  $y$  is the peak area ratio (observed peak area against that of IS) and  $x$  is the concentration (ng/mL). The limit of detection (LOD) and limit of quantification (LOQ) of M2 in db/db urine were determined as 0.12 ng/mL and 0.37

ng/mL, respectively. The LOD and LOQ of M4 in db/db urine were determined as 0.19 and 0.45 ng/mL, respectively. The standard curves of M2 and M4 in mice feces displayed superior linearity ranging from 0.1 to 500 ng/mL (M2 in the db/db feces:  $Y = 0.2088X - 1.6344$ ,  $R^2 = 0.9940$ ; M4 in the db/db feces:  $Y = 0.3931X - 3.5809$ ,  $R^2 = 0.9935$ ), where  $Y$  is the peak area ratio (observed peak area against that of IS) and  $X$  is the concentration (ng/mL). The LOD of M2 and M4 in db/db feces was determined as 0.089 and 0.031 ng/mL, respectively. And the LOQ of M2 and M4 in db/db feces was determined as 0.215 and 0.067 ng/mL, respectively. Due to the lack of standards, the concentration of M1 and M3 was expressed as M4 equivalent.

**Dose-Dependent Scavenging of MGO by Nar in Diabetic Mice.** In order to further investigate the scavenging ability of Nar on MGO in diabetic mice, mono-MGO-Nar in urine and feces was quantified by LC-MS/MS. As shown in Figure 3, there was a trend that Nar dose-dependently

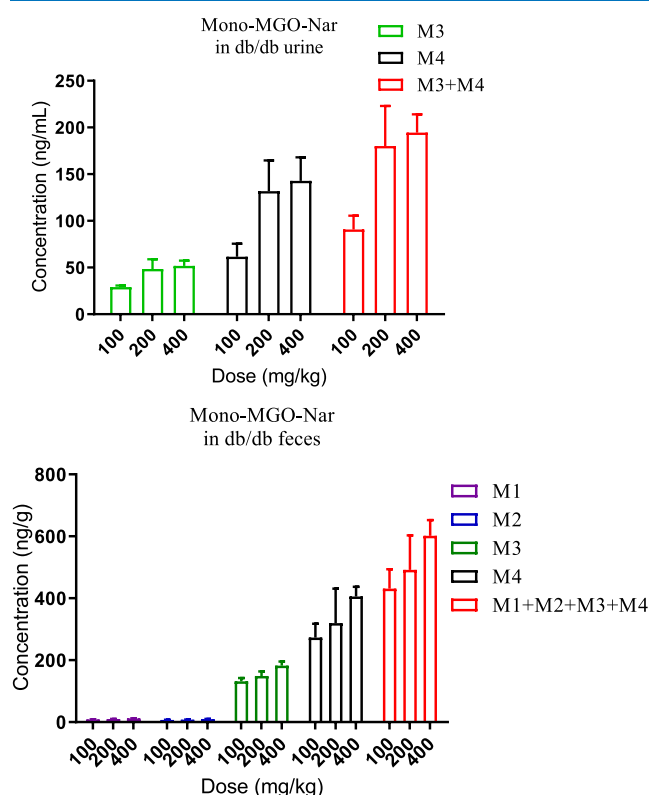


**Figure 3.** Quantification of mono-MGO-Nar in urine and fecal samples of diabetic mice after oral administration of Nar (data are shown as means  $\pm$  SD,  $n = 3$ ).

scavenged MGO in diabetic mice. The quantification analysis further confirmed that dose of Nar plays a significant role in scavenging capacity of MGO in diabetic mice.

## CONCLUSIONS

It is worth mentioning that Nar has captured the interest of scientists due to its significant anti-DKD effects through anti-inflammatory, antifibrotic, and antioxidant properties. However, it is worth considering whether Nar has scavenged MGO capacity to combat DKD. The experimental results in this paper demonstrated that Nar could scavenge MGO by the formation of mono-MGO-Nar in diabetic mice. This study

revealed a new mechanism for the anti-DKD effect of Nar, supported Nar as a lead compound of new anti-DKD drugs, and laid a foundation for its subsequent clinical research of new drugs. Although M2 and M4 have been purified and identified, future work should also continue to isolate, purify, and identify structures of M1 and M3. To the best of our knowledge, active compounds could reduce plasma MGO concentration by inhibiting MGO formation, scavenging MGO, and inducing Glo 1 expression. This project found that Nar could scavenge MGO to form monoadducts of Nar in diabetic mice. Whether Nar could inhibit MGO formation and induce Glo 1 expression should be focused on in future research. In addition, an approach should be developed in future work for studying the inhibitory capacity of Nar on the AGEs and AGEs-induced renal inflammatory injury.

## METHODOLOGY

**Chemicals.** Nar (S25634) with purity 98% were purchased from Shanghai Yuanye Biotechnology Co., Ltd. (Shanghai, China). Detailed manufacturers and batch information on MGO, 1,2-diaminobenzene (DB), 2,3-butanedione, 2,3-dimethylquinoxaline, 2-methylquinoxaline, dimethyl sulfoxide- $d_6$  (DMSO- $d_6$ ), taxifolin,  $\beta$ -glucuronidase, sulfatase, formic acid, acetonitrile, and pure distilled water have been depicted in our previous study.<sup>20</sup> Unless specified, all analytical grade reagents were bought from Shanghai Sinopharm Chemical Reagent Co., Ltd. (Shanghai, China).

**Scavenging Capacity of MGO by Nar In Vitro.** Scavenging capacity of MGO by Nar under simulated physiological conditions with molar ratios (Nar:MGO = 3:1) was assessed as previously reported.<sup>20</sup> The detailed experimental procedures are given in the Supporting Information. The reaction sample of Nar and MGO for 8 h was used as a mixture standard for identification of mono-MGO adduct of Nar in urine and feces.

**Purification of Two Mono-MGO-Nar.** Nar (0.136 g, 0.1 M) and MGO (0.1 M, 1:1) were dissolved in 10 mL of a mixture of DMSO and PBS (5/5, v/v) and then kept at 37 °C for 24 h. After the reaction, the supernatant was lyophilized and reconstituted with methanol, which was loaded onto a Sephadex LH-20 column and eluted with 100% methanol to obtain successively two mono-MGO-Nar (M2 6.56 mg; M4, 13.1 mg).

**Scavenging MGO by Nar in Diabetic Mice.** All animal studies were conducted with the approval of the Animal Ethical and Welfare Committee of the Jiangxi University of Chinese Medicine. Twelve male six-weeks-old C57BL/KsJ-db/db mice were purchased from GemPharmatech Co., Ltd. (Nanjing, China), which was bred according to ref 20. In order to study the scavenging effect of Nar on plasma MGO in diabetes mice, the experimental design was as follows: after fasting overnight, db/db mice were divided into four groups ( $n = 3$  per group): (i) db/db mice in the treatment group were treated with Nar at the dose of 100, 200, and 400 mg/kg via oral gavage based on their body weight. (ii) db/db mice in the control group received an oral administration of 0.5% CMC-Na depending on their body weight. 24 h urine and feces of all mice were collected for each mouse separately by an individual metabolic cage. Clean urine samples were achieved by centrifuging at 10,000g for 10 min. In addition, dried feces were obtained in a freeze-dryer (FD-1C-80, Shanghai, China). All samples were stored at  $-80$  °C before further analysis.



**Sample Preparation.** Preparation of urine and feces was performed based on previous studies.<sup>20</sup>

**Preparation of Calibration Samples.** The M2, M4, and IS were prepared separately at a concentration of 1 mg/mL with menthol. The working solution of IS (300 ng/mL) was obtained by the dilution of menthol. The mixed standard solution, including M3 and M4, was prepared with menthol at the concentrations of 1, 5, 10, 200, 500, 1000, 2000, 5000, 8000, and 10000 ng/mL. For calibration standards preparation in urine, 100  $\mu$ L blank urine samples were incubated with 5  $\mu$ L of  $\beta$ -glucuronidase and 4  $\mu$ L of sulfatase for 2 h at 37 °C. 10  $\mu$ L of IS (300 ng/mL) and 10  $\mu$ L of mixed standard solution of M2 and M4 (10, 200, 500, 1000, 2000, 5000, 8000, and 10000 ng/mL) were mixed and vortexed for 2 min. After adding 290  $\mu$ L of methanol to the reaction solution to precipitate the proteins, the solutions were vortexed for 3 min and centrifuged at 13,000g for 10 min at 4 °C to obtain the supernatant, which was transferred to a new clean centrifugal tube and dried under a nitrogen stream. The dried residue was reconstituted with methanol (100  $\mu$ L) and centrifuged at 13,000g for 10 min to obtain the supernatant, which was analyzed using UHPLC-QQQ-MS/MS. For calibration standards preparation in feces, 100 mg homogenized blank fecal samples were sonic extracted with 1 mL of methanol, subsequently centrifuged at 13,000g for 10 min to obtain the supernatant. 100  $\mu$ L of supernatant was added to 10  $\mu$ L of IS (300 ng/mL), and 10  $\mu$ L mixed standard solutions of M2 and M4 (1, 5, 10, 200, 500, 1000, 2000, and 5000 ng/mL) were dried under a nitrogen stream, reconstituted with methanol (100  $\mu$ L), and centrifuged at 13,000g for 10 min to obtain the supernatant, which were analyzed using UHPLC-QQQ-MS/MS.

**Instrumentation and Analytical Conditions.** The qualitative analysis of mono-MGO-Nar from the reaction between MGO and Nar, urine, and feces was carried out on a Shimadzu LC-3AD system (Shimadzu, Kyoto, Japan) coupled to an AB SCIEX Triple TOF 5600+ system mass spectrometer (AB SCIEX, Concord, Canada) with a Halo-C<sub>18</sub> column (2.1  $\times$  100 mm, 2.7  $\mu$ m). Solvent A consisted of 0.1% formic acid water and solvent B consisted of acetonitrile. The temperature of the column compartment was set at 30 °C with the chromatographic conditions as follows: starting at 5% solvent B and increasing to 10% B in 2 min, then increased to 14% B in 10 min, keeping 14% B for 3 min. For 16 min, %B was increased to 30%, then increased to 60% in 37 min and increased to 95% in 45 min, held at 95% B for 2 min, changed back to 5% in 0.1 min, and was finally isocratic until 50 min. The quantitative analysis of mono-MGO-Nar in urine and feces was carried out on the Shimadzu LC-30AD combined with an AB SCIEX QTRAP 4500 system mass spectrometer. Separation was performed using a Halo-C<sub>18</sub> column (2.1 mm  $\times$  100 mm, 2.7  $\mu$ m) and 0.1% formic acid (v/v) in water and acetonitrile as mobile phases A and B, respectively (flow rate: 0.35 mL/min). The following gradient elution program was used: 0–1 min, 15% to 30% B; 1–6 min, 30% to 30% B; 6–8 min, 30% to 100% B; 8 to 10 min, 100% to 15% B; 10–12 min, 15% to 15% B. For the MS part, the turbo ion spray source temperature was 550 °C. The ion spray voltage was assigned at 4500 V. The curtain gas was 50 psi. The ion source gas was set at 50 psi. The detection was performed in multiple reaction monitoring (MRM). The MRM transitions  $m/z$  342.9  $\rightarrow$   $m/z$  271.0 and  $m/z$  303.0  $\rightarrow$   $m/z$  125.0 were applied to quantify M2, M4, and IS, respectively. The declustering potential (DP) and collision energy (CE) of M2 and M4 were optimized as

46.21 V and 20.03 eV. And the DP and CE of IS were optimized as 108.35 V and 25.41 eV.

**NMR Analysis.** M2 and M4 were dissolved in DMSO-*d*<sub>6</sub>, and <sup>1</sup>H NMR, <sup>13</sup>C NMR, and <sup>1</sup>H–<sup>1</sup>H COSY and HMBC spectra were recorded on a Bruker AVANCE 600 MHz spectrometer (Bruker, Inc., Billerica, MA), which were processed by MestReNova (v11.0.4) software.

**Statistical Analysis of Data.** Data were reported as the mean  $\pm$  standard deviation (SD) of at least three independent experiments. Statistical significance was analyzed using GraphPad Prism 5 software (San Diego, CA, USA) by analysis of variance (ANOVA) followed by Tukey's multiple comparison test. The significant differences between different groups ( $p$  < 0.05) were marked by different letters.

## ■ ASSOCIATED CONTENT

### Supporting Information

The Supporting Information is available free of charge at <https://pubs.acs.org/doi/10.1021/acsomega.4c11440>.

Putative fragmentation pathway of mono-MGO-Nar; <sup>1</sup>H NMR, <sup>13</sup>C NMR, and HMBC data of M2; <sup>1</sup>H NMR, <sup>13</sup>C NMR, HMBC, HSQC, and <sup>1</sup>H–<sup>1</sup>H COSY data of M4; MS/MS spectra of mono-MGO-Nar in urine and fecal samples of diabetic mice after oral administration of Nar; and method for scavenging capacity of MGO by Nar in vitro (PDF)

## ■ AUTHOR INFORMATION

### Corresponding Authors

**Ting Tan** – The National Pharmaceutical Engineering Center for Solid Preparation in Chinese Herbal Medicine, Jiangxi University of Chinese Medicine, Jiangxi, Nanchang 330006, China; [orcid.org/0000-0001-8105-5422](https://orcid.org/0000-0001-8105-5422); Email: [tanting2009@126.com](mailto:tanting2009@126.com)

**Yun Luo** – Key Laboratory of Modern Preparation of Traditional Chinese Medicine, Ministry of Education, Jiangxi University of Chinese Medicine, Nanchang 330004, China; Phone: +86 791 87119632; Email: [luoyunn@163.com](mailto:luoyunn@163.com); Fax: +86 791 87119638

### Authors

**Xinxin Huang** – The National Pharmaceutical Engineering Center for Solid Preparation in Chinese Herbal Medicine, Jiangxi University of Chinese Medicine, Jiangxi, Nanchang 330006, China

**Huixian Zhou** – The National Pharmaceutical Engineering Center for Solid Preparation in Chinese Herbal Medicine, Jiangxi University of Chinese Medicine, Jiangxi, Nanchang 330006, China

Complete contact information is available at: <https://pubs.acs.org/10.1021/acsomega.4c11440>

### Author Contributions

<sup>§</sup>T.T. and Y.L. contributed equally. Xinxin Huang: Investigation, methodology, formal analysis, writing—review and editing, and writing—original draft. Huixian Zhou: Investigation, methodology, formal analysis, writing—review and editing, and writing—original draft. Ting Tan: Funding acquisition, data curation, conceptualization, project administration, writing—review and editing, and writing—original draft. Yun Luo: Data curation, conceptualization, project

administration, writing—review and editing, and writing—original draft.

## Notes

The authors declare no competing financial interest.

## ACKNOWLEDGMENTS

Financial support for this work was provided by the National Natural Science Foundation of China (No. 82260751). The study was also supported by the Jiangxi University of Chinese Medicine Science and Technology Innovation Team Development Program (No. CXTD22005).

## ABBREVIATIONS

AGEs, advanced glycation end products; CFIs, characteristic fragment ions; CMC-Na, carboxymethyl cellulose sodium; DKD, diabetic kidney disease; DMSO, dimethyl sulfoxide; EIC, extracted ion chromatogram; Glo 1, glyoxalase 1; LC-MS/MS, liquid chromatography coupled to mass spectrometry; LOD, limit of detection; LOQ, limit of quantification; MGO, methylglyoxal; MRM, multiple reaction monitoring; Nar, naringenin; NL, neutral loss; PBS, phosphate buffer solution; RDA, retro-Diels–Alder; RT, retention time; SD, standard deviation

## REFERENCES

- (1) Shen, S.; Zhong, H.; Zhou, X.; Li, G.; Zhang, C.; Zhu, Y.; Yang, Y. Advances in Traditional Chinese Medicine research in diabetic kidney disease treatment. *Pharm. Biol.* **2024**, *62* (1), 222–232.
- (2) Ma, N.; Xu, C.; Wang, Y.; Cui, K.; Kuang, H. Telomerase reverse transcriptase protects against diabetic kidney disease by promoting AMPK/PGC-1 $\alpha$ -regulated mitochondrial energy homeostasis. *Chem. Biol. Interact.* **2024**, *403*, 111238.
- (3) Zhang, X.; Jackson, S.; Liu, J.; Li, J.; Yang, Z.; Sun, D.; Zhang, W. Arsenic aggravates the progression of diabetic nephropathy through miRNA-mRNA-autophagy axis. *Food Chem. Toxicol.* **2024**, *187*, 114628.
- (4) Matafome, P.; Sena, C.; Seica, R. Methylglyoxal, obesity, and diabetes. *Endocrine* **2013**, *43* (3), 472–484.
- (5) Schalkwijk, C. G.; Stehouwer, C. D. Methylglyoxal, a highly reactive dicarbonyl compound, in diabetes, its vascular complications, and other age-related diseases. *Physiol. Rev.* **2020**, *100* (1), 407–461.
- (6) Kalapos, M. P. Where does plasma methylglyoxal originate from? *Diabetes Res. Clin. Pract.* **2013**, *99* (3), 260–271.
- (7) Lai, S. W. T.; Hernandez-Castillo, C.; Gonzalez, E. J. L.; Zoukari, T.; Talley, M.; Paquin, N.; Chen, Z.; Roep, B. O.; Kaddis, J. S.; Natarajan, R.; Termini, J.; Shuck, S. C. Methylglyoxal adducts are prognostic biomarkers for diabetic kidney disease in patients with type 1 diabetes. *Diabetes* **2024**, *73* (4), 611–617.
- (8) Tan, S. M.; Lindblom, R. S. J.; Ziemann, M.; Laskowski, A.; Granata, C.; Snelson, M.; Thallas-Bonke, V.; El-Osta, A.; Baeza-Garza, C. D.; Caldwell, S. T.; Hartley, R. C.; Krieg, T.; Cooper, M. E.; Murphy, M. P.; Coughlan, M. T. Targeting methylglyoxal in diabetic kidney disease using the mitochondria-targeted compound MitoGamide. *Nutrients* **2021**, *13* (5), 1457.
- (9) Azegami, T.; Nakayama, T.; Hayashi, K.; Hishikawa, A.; Yoshimoto, N.; Nakamichi, R.; Itoh, H. Vaccination against receptor for advanced glycation end products attenuates the progression of diabetic kidney disease. *Diabetes* **2021**, *70* (9), 2147–2158.
- (10) Zhou, Q.; Cheng, K. W.; Xiao, J. B.; Wang, M. F. The multifunctional roles of flavonoids against the formation of advanced glycation end products (AGEs) and AGEs-induced harmful effects. *Trends Food Sci. Technol.* **2020**, *103*, 333–347.
- (11) Zhou, H. X.; Huang, X. X.; Luo, Y.; Tan, T. Scavenging of methylglyoxal by the total flavonoids of *Apocyni Veneti Folium* in mice. *J. Agric. Food Chem.* **2024**, *72* (37), 20374–20382.
- (12) Zhang, S.; Xiao, L.; Lv, L. S.; Sang, S. Trapping methylglyoxal by myricetin and its metabolites in mice. *J. Agric. Food Chem.* **2020**, *68* (35), 9408–9414.
- (13) Li, X.; Zheng, T.; Sang, S. M.; Lv, L. S. Quercetin inhibits advanced glycation end product formation by trapping methylglyoxal and glyoxal. *J. Agric. Food Chem.* **2014**, *62* (50), 12152–12158.
- (14) Zhao, Y.; Tang, Y.; Sang, S. Dietary quercetin reduces plasma and tissue methylglyoxal and advanced glycation end products in healthy mice treated with methylglyoxal. *J. Nutr.* **2021**, *151* (9), 2601–2609.
- (15) Zheng, L.; Bakker, W.; Estruch, I. M.; Widjaja, F.; Rietjens, I. M. C. M. Comparison of the methylglyoxal scavenging effects of kaempferol and glutathione and the consequences for the toxicity of methylglyoxal in SH-SY5Y cells. *Food Chem. X* **2023**, *20*, 100920.
- (16) Wang, P.; Chen, H.; Sang, S. Trapping methylglyoxal by genistein and its metabolites in mice. *Chem. Res. Toxicol.* **2016**, *29* (3), 406–414.
- (17) Zhao, Y.; Zhu, Y.; Wang, P.; Sang, S. Dietary genistein reduces methylglyoxal and advanced glycation end product accumulation in obese mice treated with high-fat diet. *J. Agric. Food Chem.* **2020**, *68* (28), 7416–7424.
- (18) Shao, X.; Bai, N.; He, K.; Ho, C. T.; Yang, C. S.; Sang, S. Apple polyphenols, phloretin and phloridzin: new trapping agents of reactive dicarbonyl species. *Chem. Res. Toxicol.* **2008**, *21* (10), 2042–2050.
- (19) Zhu, D.; Wang, L.; Zhou, Q.; Yan, S.; Li, Z.; Sheng, J.; Zhang, W. (+)-Catechin ameliorates diabetic nephropathy by trapping methylglyoxal in type 2 diabetic mice. *Mol. Nutr. Food Res.* **2014**, *58* (12), 2249–2260.
- (20) Zhang, Y.; Zhan, L.; Wen, Q.; Feng, Y.; Luo, Y.; Tan, T. Trapping methylglyoxal by taxifolin and its metabolites in mice. *J. Agric. Food Chem.* **2022**, *70* (16), S026–S038.
- (21) Sang, S.; Shao, X.; Bai, N.; Lo, C. Y.; Yang, C. S.; Ho, C. T. Tea polyphenol (–)-epigallocatechin-3-gallate: a new trapping agent of reactive dicarbonyl species. *Chem. Res. Toxicol.* **2007**, *20* (12), 1862–1870.
- (22) Thilavech, T.; Marnpae, M.; Mäkinen, K.; Adisakwattana, S. Phytochemical composition, antiglycation, antioxidant activity and methylglyoxal-trapping action of Brassica Vegetables. *Plant Foods Hum. Nutr.* **2021**, *76* (3), 340–346.
- (23) Yan, N.; Wen, L.; Peng, R.; Li, H.; Liu, H.; Peng, H.; Sun, Y.; Wu, T.; Chen, L.; Duan, Q.; Sun, Y.; Zhou, Q.; Wei, L.; Zhang, Z. Naringenin ameliorated kidney injury through Let-7a/TGFBR1 signaling in diabetic nephropathy. *J. Diabetes Res.* **2016**, *2016*, 1–13.
- (24) Ding, S.; Qiu, H.; Huang, J.; Chen, R.; Zhang, J.; Huang, B.; Zou, X.; Cheng, O.; Jiang, Q. Activation of 20-HETE/PPARs involved in reno-therapeutic effect of naringenin on diabetic nephropathy. *Chem. Biol. Interact.* **2019**, *307*, 116–124.
- (25) Valle-Velázquez, E.; Zambrano-Vásquez, O. R.; Cortés-Camacho, F.; Sánchez-Lozada, L. G.; Guevara-Balcázar, G.; Osorio-Alonso, H. Naringenin-a potential nephroprotective agent for diabetic kidney disease: A comprehensive review of scientific evidence. *Biomol. Biomed.* **2024**, *24* (6), 1441–1451.
- (26) Nguyen-Ngo, C.; Willcox, J. C.; Lappas, M. Anti-diabetic, anti-inflammatory, and anti-oxidant effects of naringenin in an in vitro human model and an in vivo murine model of gestational diabetes mellitus. *Mol. Nutr. Food Res.* **2019**, *63* (19), 1900224.
- (27) Zhu, H.; Poojary, M. M.; Andersen, M. L.; Lund, M. N. Effect of pH on the reaction between naringenin and methylglyoxal: A kinetic study. *Food Chem.* **2019**, *298*, 125086.
- (28) Liu, P.; Yin, Z.; Chen, M.; Huang, C.; Wu, Z.; Huang, J.; Ou, S.; Zheng, J. Cytotoxicity of adducts formed between quercetin and methylglyoxal in PC-12 cells. *Food Chem.* **2021**, *352*, 129424.